Determination of hyperfine structure constants of $5D_{5/2}$ and $7S_{1/2}$ states of rubidium in cascade atomic system

Shaohua Li (李少华)[1,2], Yihong Li (李一鸿)[1,2], Jinpeng Yuan (元晋鹏)[1,2,*],
Lirong Wang (汪丽蓉)[1,2,**], Liantuan Xiao (肖连团)[1,2], and Suotang Jia (贾锁堂)[1,2]

[1]*State Key Laboratory of Quantum Optics and Quantum Optics Devices, Institute of Laser Spectroscopy,*
Shanxi University, Taiyuan 030006, China
[2]*Collaborative Innovation Center of Extreme Optics, Shanxi University, Taiyuan 030006, China*
*Corresponding author: yjp@sxu.edu.cn; **corresponding author: wlr@sxu.edu.cn
Received January 26, 2018; accepted April 3, 2018; posted online May 30, 2018

We present a method to precisely determine the hyperfine structure constants of the rubidium $5D_{5/2}$ and $7S_{1/2}$ states in a cascade atomic system. The probe laser is coupled to the $5S_{1/2} \rightarrow 5P_{3/2}$ hyperfine transition, while the coupling laser is scanned over the $5P_{3/2} \rightarrow 5D_{5/2}(7S_{1/2})$ transition. The high-resolution double-resonance optical pumping spectra are obtained with two counter-propagating laser beams acting on rubidium vapor. The hyperfine splitting structures are accurately measured by an optical frequency ruler based on the acousto-optic modulator, thus, the magnetic dipole hyperfine coupling constant A and quadrupole coupling constant B are determined. It is of great significance for the atomic hyperfine structure and fundamental physics research.

OCIS codes: 020.2930, 300.6210.
doi: 10.3788/COL201816.060203.

The measurement of hyperfine splitting structures of alkali atoms at an excited state is important for electron–nucleus interaction[1], atomic parity non-conservation[2], precision measurement of fundamental constants[3,4], high-resolution laser spectroscopy[5], optical frequency standards, and optical frequency measurement[6,7]. For the excited states of Rb atoms, the 5D and 7S states have attracted more and more interest from researchers. For the 5D states, the small energy difference between the two transitions induces a high-transition probability and a better Doppler-free background. The relatively narrow natural linewidth and lower sensitivity to the external environment make the state a good candidate for establishing optical frequency standards with high stability[8]. For the 7S state, the $5S \rightarrow 5P \rightarrow 7S$ transition is less sensitive to magnetic fields, since both $5S_{1/2}$ and $7S_{1/2}$ states have the same Landé g-factor, and the linear Zeeman shift is zero[9], which makes it widely used in precision measurement.

The Doppler-free double-photon spectroscopy[10], optical double-resonance spectroscopy[11], resonance-enhanced ionization spectroscopy[12], cascade radio-frequency spectroscopy[13], and electromagnetically induced transparency spectroscopy[14] are used to determine the hyperfine structure constants. Compared with these methods, the double-resonance optical pumping (DROP) spectroscopy has a higher signal-to-noise ratio for detecting the population of the ground state instead of the excited states. Especially for Rb atoms, the intermediate $5P_{3/2}$ state has high spontaneous emission rate, which will accelerate the DROP process[15].

For the calibration of the spectrum components, the Fabry–Perot (FP) cavity, electro-optic modulator (EOM), and acousto-optic modulator (AOM) are often used as the frequency rulers. The accuracy of the FP cavity is limited by thermal fluctuations and mechanical vibrations. The EOM frequency ruler also needs the FP cavity as the auxiliary tool, which will make the system complicated. The AOM can be driven by an easily measured and constructed radio-frequency source, which has the accuracy of 1×10^{-6} and an error of less than 1 kHz introduced into the frequency scale[16]. It is relatively free of large systematic effects and leads to a higher precision in the hyperfine splitting structure measurement.

In this Letter, we determine the hyperfine structure constants of the $5D_{5/2}$ and $7S_{1/2}$ states of Rb atoms with DROP spectroscopy, which is calibrated by the AOM frequency ruler. When the coupling laser is tuned to the $5P_{3/2} \rightarrow 5D_{5/2}(7S_{1/2})$ transition, and the probe laser is locked to the $5S_{1/2} \rightarrow 5P_{3/2}$ transition, we obtain high-resolution DROP spectra. The hyperfine splitting structures of the $5D_{5/2}$ and $7S_{1/2}$ states of the two isotopes ^{85}Rb and ^{87}Rb are measured, and thus, the hyperfine structure constants are determined. This work is important for the development of precision measurement.

The relevant hyperfine energy levels of the two isotopes ^{85}Rb and ^{87}Rb are illustrated in Fig. 1. The nuclear spin quantum numbers of ^{87}Rb and ^{85}Rb are 3/2 and 5/2, respectively. The probe laser operating at 780 nm is resonant on the $5S_{1/2} \rightarrow 5P_{3/2}$ transition, while the coupling laser is tuned to the upper $5P_{3/2} \rightarrow 5D_{5/2}(7S_{1/2})$ transition at 776 nm (741 nm).

The experimental setup is schematically depicted in Fig. 2. The coupling laser is provided by a Ti:sapphire laser system (SolaTis-SRX-XF, M Squared Lasers), which can be tuned from 600 to 1000 nm. The wavelength of the laser can be monitored by a wavelength meter (WS-7, HighFinesse). The coupling laser is divided into two beams by the AOM, and then zeroth-order and first-order laser beams are recombined together by the
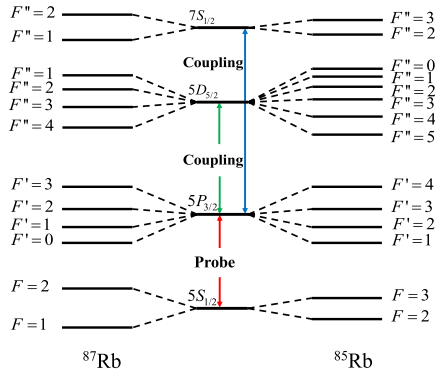
Fig. 1. Energy-level diagram of the $5S_{1/2} \rightarrow 5P_{3/2} \rightarrow 5D_{5/2}$ and $5S_{1/2} \rightarrow 5P_{3/2} \rightarrow 7S_{1/2}$ transitions of ^{87}Rb$\,(I = 3/2)$ and ^{85}Rb$\,(I = 5/2)$. The total angular values are given (not scaled).
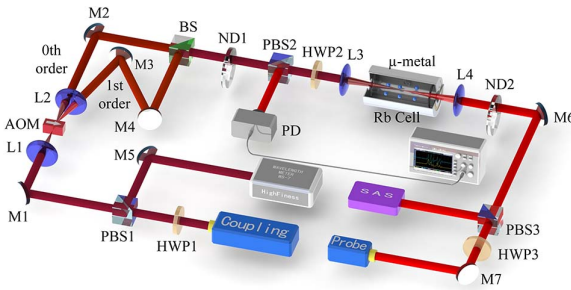

Fig. 2. Experimental setup. ND, neutral density plate; M, mirror; L, lens; AOM, acousto-optic modulator; BS, beam splitter; PBS, polarizing beam splitter; HWP, half-wave plate; PD, Si photodiode; OSC, oscilloscope.

beam splitter (BS). The laser power can be adjusted by a neutral density plate (ND1). The probe laser operating at 780 nm is derived from a single mode tunable diode laser (DL pro, Toptica). The linewidth is less than 1 MHz after being stabilized by the saturation absorption spectroscopy. The probe laser beam and coupling laser beam with counter-propagation configuration have identical linear polarization. The vapor cell is 2.5 cm in diameter and 10 cm in length and placed in a μ-metal shield box. The focused probe laser beam and coupling laser beam in the center of the vapor cell are about 100 μm. The transmission signal of the probe laser beam is detected by a Si photodiode detector (PDA36A-EC, Thorlabs).

The DROP spectra of different transitions and the corresponding differential signals are shown in Fig. 3. The blue curves in the lower part of the figure are the DROP spectra of different transitions, and the red curves in the upper part are the corresponding differential signals. The differential signals are obtained by phase sensitivity detection. The frequency interval of the two components, which are labeled as the zeroth-order and first-order, is 100 MHz. Figure 3(a) shows the $5S_{1/2}(F = 2) \rightarrow$ $5P_{3/2}(F = 3) \rightarrow 5D_{5/2}$ $(F = 2, 3$ and 4) transitions of ^{87}Rb. The three peaks correspond to $5S_{1/2}(F = 2) \rightarrow 5P_{3/2}$ $(F = 3) \rightarrow 5D_{5/2}$ $(F = 4, 3$ and 2) from left to right, which are represented as 2-3-4, 2-3-3, and 2-3-2, respectively.
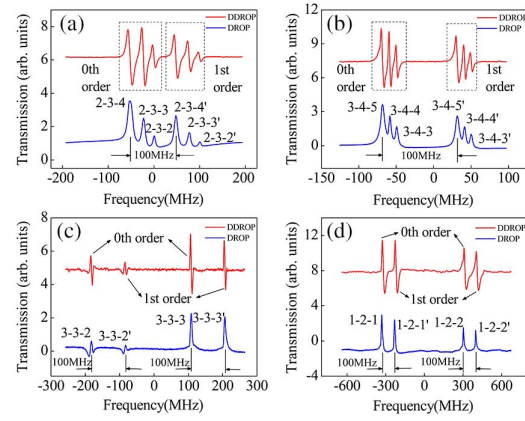

Fig. 3. Double-resonance optical pumping spectra (the lower curve) and corresponding differential signals (the upper curve). (a) $5S_{1/2}(F = 2) \rightarrow 5P_{3/2}(F = 3) \rightarrow 5D_{5/2}$ $(F = 2, 3$ and 4) transitions of ^{87}Rb. (b) $5S_{1/2}(F = 3) \rightarrow 5P_{3/2}(F = 4) \rightarrow 5D_{5/2}$ $(F = 3, 4$ and 5) transitions of ^{85}Rb. (c) $5S_{1/2}(F = 3) \rightarrow$ $5P_{3/2}(F = 3) \rightarrow 7S_{1/2}$ $(F = 2$ and 3) transitions of ^{85}Rb. (d) $5S_{1/2}(F = 1) \rightarrow 5P_{3/2}(F = 2) \rightarrow 7S_{1/2}$ $(F = 1$ and 2) transitions of ^{87}Rb.

Figure 3(b) shows the $5S_{1/2}(F = 3) \rightarrow 5P_{3/2}(F = 4) \rightarrow$ $5D_{5/2}$ $(F = 3, 4$ and 5) transitions of ^{85}Rb. The excitation rate of the $5S_{1/2} \rightarrow 5P_{3/2} \rightarrow 7S_{1/2}$ transition is estimated to be ∼100 times smaller than that of the $5D_{5/2}$ state for the ∼20 nm detuning from the $5P_{3/2}$ intermediate state, which makes it difficult to measure the hyperfine structure[17]. We also obtain the $5S_{1/2} \rightarrow 5P_{3/2} \rightarrow 7S_{1/2}$ transitions of ^{85}Rb and ^{87}Rb, which are shown in Figs. 3(c) and 3(d). The hyperfine splitting structures are determined by fitting the differential signals with the differential form of a multipeak Voigt function. Take Fig. 3(a) as an example. Since the coupling laser is divided into two beams with the same parameters but with a fixed frequency shift of 100 MHz, the frequency interval of transition 2-3-4 to 2-3-4' (2-3-3 to 2-3-3', 2-3-2 to 2-3-2') is 100 MHz. With this frequency ruler, we can measure the frequency interval of the hyperfine transition 2-3-4 to 2-3-3 and 2-3-3 to 2-3-2 of the ^{87}Rb $5D_{5/2}$ state as 29.282 and 23.289 MHz, respectively. The frequency interval of the hyperfine transition 3-4-5 to 3-4-4 and 3-4-4 to 3-4-3 of the ^{85}Rb $5D_{5/2}$ state can be obtained from Fig. 3(b) as 9.781 and 9.079 MHz, respectively. For the $7S_{1/2}$ state, the hyperfine transition 3-3-2 to 3-3-3 of ^{85}Rb is determined as 291.090 MHz from Fig. 3(c), and the frequency interval of the hyperfine transition 1-2-1 to 1-2-2 of ^{87}Rb is determined as 639.228 MHz from Fig. 3(d).

The hyperfine structure originates from the interaction of the nuclear moments with atomic electrons moments. The Hamiltonian for the electron-nuclear system interaction is represented as follows[18]:

$$H_{\mathrm{hfs}} = A \cdot I \cdot J + B \frac{3(I \cdot J)^2 \times \frac{3}{2}(I \cdot J) - I(I+1)J(J+1)}{2I(2I-1)J(2J-1)},$$

$$(1)$$

Table 1. Hyperfine Coupling Constants A and B of the $5D_{5/2}$ and $7S_{1/2}$ States of ^{87}Rb and ^{85}Rb[a]

Reference	Method	State	^{85}A	^{85}B	^{87}A	^{87}B
1975, Gupta et al.[19]	Theory	$5D_{2/5}$	1.71		5.81	
1995, Grove et al.[11]	Optical double-resonance spectroscopy		−2.196	2.51	−7.45	0.462
1999, Gabbanini et al.[12]	Resonance-enhanced ionization spectroscopy		−2.31	2.7	−7.51	2.7
This work	DROP spectroscopy		−2.23	2.32	−7.57	1.26
1973, Tai et al.[13]	Theory	$7S_{1/2}$	97.58	–	330.7	–
1996, Snadden et al.[17]	Two-photon spectroscopy		94.7	–	319.7	–
2005, Krishna et al.[14]	Electromagnetically induced transparency spectroscopy		94.085	–	319.174	–
This work	DROP spectroscopy		97.03	–	319.61	–

[a]unit: MHz.

where A is the magnetic dipole constant, B is the electric quadrupole constant, I is the nuclear spin angular momentum quantum number, and J is the total electron angular momentum quantum number. The total atomic angular moment is $F = I + J$.

The eigen energy under the hyperfine interaction can be expressed in terms of the hyperfine energy shift:

$$\Delta E_{\mathrm{hfs}} = A \cdot F + B \frac{\frac{3}{2} F[F^2 - I(I+1) - J(J+1) + \frac{1}{2}]}{I(2I-1)J(2J-1)}. \quad (2)$$

Using Eq. (2) and the hyperfine structure splitting measured from the Figs. 3(a)–3(d), the magnetic dipole hyperfine coupling constants A and quadrupole coupling constants B of the $5D_{5/2}$ state and $7S_{1/2}$ state of ^{87}Rb and ^{85}Rb are determined, which are shown in Table 1. From the Table 1, we can get the information that an accuracy theoretical calculation is difficult for hyperfine structure constants. The results obtained in this work by DROP spectroscopy in a thermal atomic system coincide with the previous results. A more accurate measurement is needed in the future by considering more influencing factors. The error of the results is considered to be less than 50 kHz. Several possible systematic uncertainties contribute to the error, such as nonlinearity of the frequency scanning, the accuracy in determining the structure, AC-Stark frequency shift, Zeeman frequency shift, misalignments of two lasers, and frequency drift of probe laser. Theoretically, the AC-Stark frequency shifts are almost the same for each hyperfine component of the same state and cause no effect on the hyperfine splitting measurement, because the relative interval is used instead of the absolute frequency. In fact, the hyperfine structures are slightly affected when the laser power changes. For the operating power of the measurement, the AC-Stark frequency shift is estimated to be less than 5 kHz. The Zeeman shift is eliminated by perfectly linearly polarized laser beams and a μ-metal box to shield the stray magnetic field, and thus, the value is reduced to be negligible for the result. Misalignment of the two beams will shift the peaks, but since the atomic velocity distribution is isotropic, the peaks shift in the same direction with equal frequency. The error brought by the misalignment is estimated to be less than 1 kHz. The error caused by frequency drift of the probe laser can be eliminated by repeated measurements. The main possible systematic error comes from the accuracy in determining the hyperfine structure by fitting the experimental spectrum with the theoretical model, which is less than 30 kHz.

In conclusion, we obtain the high-resolution DROP spectra of the rubidium $5D_{5/2}$ and $7S_{1/2}$ states. The hyperfine structure splitting of $5D_{5/2}(7S_{1/2})$ is accurately calibrated by an AOM frequency ruler. The magnetic dipole hyperfine coupling constant A and quadrupole coupling constant B are determined. This work provides a convenient technique to measure the hyperfine structure of excited states, which is very important for parity nonconservation and related research.

References
1. V. Natarajan, *Modern Atomic Physics* (CRC Press, 2015).
2. C. S. Wood, S. C. Bennett, D. Cho, B. P. Masterson, J. L. Roberts, C. E. Tanner, and C. E. Wieman, Science **275**, 1759 (1997).
3. S. Bize, Y. Sortais, and M. S. Santos, Europhys. Lett. **45**, 558 (1999).
4. G. H. Yu, H. Yan, J. Q. Zhong, H. Liu, X. L. Zhu, and W. Yang, Mod. Phys. Lett. B **32**, 1750359 (2018).
5. Y. P. Gangrskii, S. G. Zemyanoi, and B. N. Markov, Meas. Tech. **40**, 577 (1997).

6. T. J. Quinn, Metrologia **40**, 103 (2003).

7. P. Y. Chang, T. T. Shi, S. N. Zhang, H. S. Shang, D. Pan, and J. B. Chen, Chin. Opt. Lett. **15**, 121401 (2017).

8. M. Zhu and R. W. Standridge, Opt. Lett. **22**, 730 (1997).

9. N. D. Zameroski, G. D. Hager, C. J. Erickson, and J. H. Burke, J. Phys. B **47**, 225205 (2014).

10. F. Nez, F. Biraben, R. Felder, and Y. Millerioux, Opt. Commun. **102**, 432 (1993).

11. T. T. Grove, V. Sanchez-Villicana, B. C. Duncan, S. Maleki, and P. L. Gould, Phys. Scr. **52**, 271 (1995).

12. C. Gabbanini, F. Ceccherini, S. Gozzini, and A. Lucchesini, Meas. Sci. Technol. **10**, 772 (1999).

13. C. Tai, W. Happer, and R. Gupta, Phys. Rev. A **12**, 736 (1975).

14. A. Krishna, K. Pandey, A. Wasan, and V. Natarajan, Europhys. Lett. **72**, 221 (2005).

15. D. Sheng, A. Pérez Galván, and L. A. Orozco, Phys. Rev. A **78**, 062506 (2008).

16. Y. K. Luo, S. H. Yan, A. A. Jia, C. H. Wei, Z. H. Li, E. L. Wang, and J. Yang, Chin. Opt. Lett. **14**, 121401 (2016).

17. M. J. Snadden, A. S. Bell, E. Riis, and A.I. Ferguson, Opt. Commun. **125**, 70 (1996).

18. C. J. Foot, *Atomic Physics* (Oxford University, 2005).

19. R. Gupta, W. Happer, L. K. Lam, and S. Svanberg, Phys. Rev. A **8**, 2792 (1973).